Diffusion and local deconfinement in relativistic systems

Georg Wolschin*
Institut für Theoretische Physik der Universität, D-69120 Heidelberg, Germany
(Received 4 September 2002; revised manuscript received 18 August 2003; published 27 February 2004)

In relativistic heavy-ion systems at the highest collision energies, new deconfinement signatures emerge and indicate an increasingly clear separation between soft hadronic processes and hard partonic interactions in a locally deconfined subsystem. Here the emphasis is on longitudinal variables, namely, net-baryon rapidity distributions. As described in a Relativistic Diffusion Model, they change from bell shaped at the lower to double humped at the higher SPS energy, but do not reach local statistical equilibrium. At $\sqrt{s_{NN}}=200$ GeV in the Au-Au system, however, they are shown to consist of three components. In addition to the nonequilibrium contributions, a third fraction close to midrapidity containing $Z_{eq}\simeq 22$ protons reaches local statistical equilibrium in a discontinuous transition. It may be associated with a deconfinement of the participant partons and thus, serve as a signature for quark-gluon matter formation.

DOI: 10.1103/PhysRevC.69.024906 PACS number(s): 25.75.−q, 24.60.Ky, 24.10.Jv, 05.40.−a

I. INTRODUCTION

Considerable progress has recently been made in the long-standing attempts [1] to recreate a quark-gluon plasma under laboratory conditions by means of relativistic heavy-ion collisions. Quark matter is believed to constitute an important intermediate state of the very early universe. There it is in thermal equilibrium, but expands, cools, and ends in the most dramatic event of a quark-hadron phase transition—a thermal confinement transition—at about 10μs: quarks and gluons condense to form a gas of nucleons and light mesons, the latter decaying afterwards.

As the temperature drops to about 170 MeV, the hadron gas becomes sufficiently dilute, and the hadron abundances for different particle species remain fixed ("chemical freeze-out"). The phase transition has thus set the stage for the subsequent primordial synthesis of light nuclei (d, He-3, He-4, Li-7) at times $t\simeq 1$ s, and temperatures $T\simeq 1$ MeV in the evolution of the early universe [2].

The attempt to investigate the quark-hadron phase transition in reverse order, as a deconfinement transition, together with the subsequent confinement transition in the laboratory by means of relativistic heavy-ion collisions experiences severe difficulties. The system has to be sufficiently extended, small collision partners such as protons or deuterons are not suitable. The energy density has to reach values above the critical one (about 1.5 GeV/fm^3) for the transition to occur.

The typical time scale for relativistic heavy-ion collisions in the laboratory is only about 10^{-23} s—to be compared with the much larger time scale of the cosmological QCD transition of 10^{-5} s. Hence, it cannot be expected that thermal equilibrium, which governs the physical description of the early universe, remains a valid concept for theoretical models of relativistic heavy-ion collisions. Whereas particle abundances have been shown to be described rather accurately by phase-space ("thermal") models [3–5], this does not necessarily imply that the system has reached, or gone through, thermal equilibrium. Instead, one has to look for stages of *local* kinetic equilibrium in the short time evolution of the system, and for the possibility that the deconfinement transition occurs in such a stage of local thermal equilibrium, affecting only a relatively small number of nucleons in a relatively big system.

In the fixed-target experiments at the SPS with heavy systems—in particular, with the Pb-Pb system at $\sqrt{s_{NN}}=17.3$ GeV—a number of possible phase-transition signatures such as strangeness enhancement and excess of dileptons with invariant mass below that of the ρ meson had been discussed. The most promising signal, namely, the suppressed production of the J/Ψ meson in the presence of a quark-gluon plasma due to vanishing string tension and screening, had been predicted by theorists [6] and identified at the SPS in heavy systems, but since it could also be caused by hadronic final-state interactions (nuclear absorption) it seemed not fully convincing.

Whether the "extra suppression" which was then detected in the Pb-Pb system at $\sqrt{s_{NN}}=17.3$ GeV and which could not easily be accounted for by absorption constitutes a qgp signature is still a matter of debate. At the relativistic heavy-ion collision (RHIC) energy of 200 GeV per particle, the PHENIX Collaboration has presented preliminary results for the J/Ψ-meson [7] showing a slight suppression. In view of the large error bars, however, this is not yet conclusive either, one has to wait for more precise data.

In a probably more promising effort, the four RHIC Au-Au experiments have carefully investigated the particle production in central collisions at high transverse momenta. When compared to p-p data that are scaled with the number of binary collisions, a significant suppression of the produced hadrons is found, which is interpreted as a final-state effect of the produced dense medium—and possibly, of a quark-gluon plasma. The effect may be due to "jet quenching": energetic partons traversing the dense medium lose energy or are completely absorbed, and the remaining observed hadronic jets are mostly created from partons produced near the surface and directed outwards.

The effect is not observed (instead, the inclusive yield is

*Email address: wolschin@uni-hd.de http://wolschin.uni-hd.de

slightly enhanced) in the lighter d-Au system, where compression and heating is much less pronounced, and where qgp formation is therefore unlikely [8–11]. Moreover, back-to-back pairs are also strongly suppressed in central Au-Au for similar reasons, whereas near-side pairs exhibit jetlike correlations that are similar to *p-p* and d-Au results, also pointing towards jet absorption in the dense (qgp?) medium [12].

Whereas these results focus essentially on transverse variables, longitudinal variables also offer very interesting conclusions regarding hadronic vs partonic interactions, and the possibility of qgp formation. In this contribution, I shall therefore concentrate on longitudinal variables—in particular, rapidity distributions of net baryons. The analysis is based on a Relativistic Diffusion Model (RDM) that allows to deal with analytical solutions, rather than numerical codes that often provide little insight into the physical assumptions.

II. RELATIVISTIC DIFFUSION MODEL

The Relativistic Diffusion Model emphasizes the nonequilibrium-statistical features of relativistic heavy-ion collisions. It also encompasses kinetic (thermal) equilibrium of the system for times that are sufficiently larger than the relaxation times of the relevant variables such as transverse energy $E_\perp$ or rapidity y.

A first (linear) version of the RDM had been proposed in 1996 and applied successfully to the analysis of AGS and SPS data, with an emphasis on transverse energy distributions integrated over all particle species, and the mean value of the rapidity as function of transverse energy [13]. Although transverse energy spectra of produced particles turn out to be close to thermal equilibrium, some deviations from equilibrium appear in the transverse variables. Based on analytical solutions of a transport equation, accurate predictions of transverse energy spectra were made, such as in case of the Pb-Pb system at the highest SPS energy.

Distributions of longitudinal variables are of greater interest in the RDM-approach since they remain farther away from thermal equilibrium. This is particularly true for the rapidity $y=1/2\ \ln((E-p)/(E-p))$, which is the Lorentz-invariant counterpart of the velocity in the beam direction at relativistic energies. Hence, I have focussed the RDM in 1999 on rapidity distributions [14]. For net (participant) baryons, δ-function initial conditions corresponding to the beam rapidities are appropriate, and analytical solutions of the rapidity transport equation can be compared with data for net-proton rapidity spectra.

Although the initial conditions are less straightforward for produced hadrons, Biyajima *et al.* have started in 2002 [15] to use the analytical RDM—which they had developed independently from, but with exactly the same result as in Refs. [14,16]—for produced hadrons. Comparing to a vast amount of RHIC data for produced charged hadrons (PHOBOS and BRAHMS) at both 130 GeV and 200 GeV center-of-mass energy per particle pair, they obtain high-precision fits of the data with adjusted values of the friction coefficient (rapidity relaxation time in my terminology) and the variance (rapidity diffusion coefficient) [15,17]. With the RDM approach, they are also able to relate pseudorapidity and rapidity distributions to each other, and to establish scaling of the charged-particle rapidity distributions with the number of charged hadrons (rather than the number of participants, or binary collisions).

Based on rapidity diffusion coefficients that are not fitted, but instead calculated analytically using a dissipation-fluctuation theorem in the weak-coupling limit (where the time between two subsequent interactions is large compared to the duration of an individual interaction), in 1999 I have obtained good RDM results for net-proton distributions at the low SIS energies of about 1 GeV per particle. However, this limit is not attained at AGS and SPS energies, where progressively larger deviations between RDM weak-coupling result and data occur [16]. These deviations have been confirmed in an independent numerical calculation by Lavagno in 2002 [18].

Two solutions of this problem have been offered so far. In a strong-coupling treatment, the diffusion coefficient D_y in rapidity space becomes time dependent [16,19]. For certain parametrizations of $D_y(t)$, analytical solutions of the RDM are still possible. As a simple substitute in comparisons with data, the enhancement factor due to multiparticle (collective) effects may be determined from the deviation between weak-coupling solution and data. Typical results for net-proton rapidity distributions at the lower SPS beam momentum of 40 GeV/c, the higher SPS beam momentum of 158 GeV/c per particle, and RHIC (100 GeV/c per particle in each beam) are shown in Fig. 1.

Alternatively, one may resort to nonextensive statistics, with the underlying relativistic diffusion equation in rapidity space becoming nonlinear. This approach has been used by Alberico *et al.* in 2000 for transverse mass spectra and transverse momentum fluctuations at SPS energies, assuming that they were in statistical equilibrium [20]. In view of the discrepancy between the nonequilibrium weak-coupling result and the SPS Pb-Pb data, the approach has been extended to the nonequilibrium situation in rapidity space, where Tsallis' nonextensivity parameter [21] q has been determined from the 158*A* GeV Pb-Pb data [18]. Whereas this may well be a reasonable phenomenological parametrization of the data, it appears to cover up the multiparticle effects which emerge explicitly in the linear approach when comparing data and weak-coupling dissipation-fluctuation theorem.

Subsequently both the linear (extensive) and the nonlinear (nonextensive) approach to nonequilibrium processes in relativistic many-body systems are pursued further, with an emphasis on the most recent high-energy results which are investigated experimentally at RHIC. I concentrate here on net baryons, and refer the reader to Biyajima *et al.* for produced hadrons in the linear RDM [15,17,22].

III. NET BARYON RAPIDITY SPECTRA

Rapidity distributions of participant (net) baryons are very sensitive to the dynamical and statistical properties of nucleus-nucleus collisions at high energies. Recent results for net-proton rapidity spectra in central Au+Au collisions at the highest RHIC energy of $\sqrt{s_{NN}}=200$ GeV show an unex-

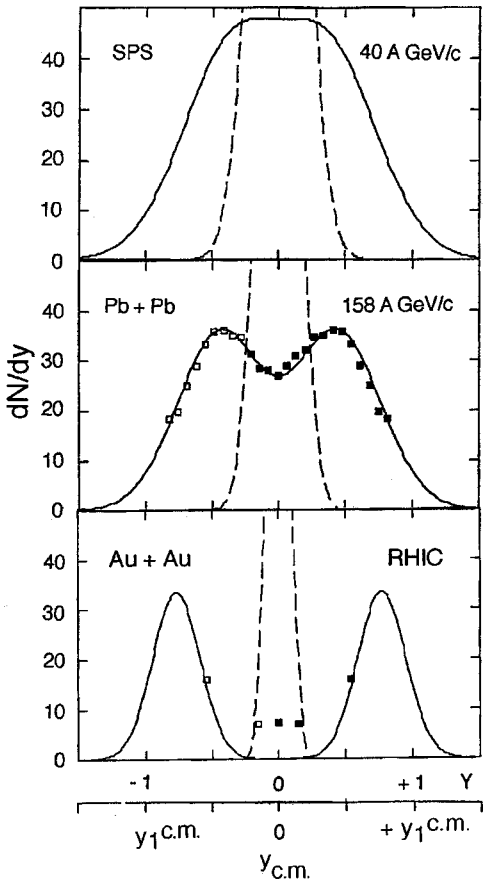

FIG. 1. Net-proton rapidity spectra in the RDM, solid curves, at the lower SPS momentum of 40 GeV/c per particle (top; data not yet available), at 158 GeV/c (compared to NA 49 data [38]; cf. Fig. 6 for error bars) and at the highest RHIC energy $\sqrt{s_{NN}}=200$ GeV (compared to preliminary BRAHMS data [23]). The variable $Y=y/y_b$ renormalizes the y distributions in the center of mass with the beam rapidities $\pm y_b$. Dashed lines are thermal equilibrium results without expansion. The transition from bell shaped to double humped is clearly shown in the RDM.

pectedly large rapidity density at midrapidity. The BRAHMS Collaboration finds [23] $dN/dy=7.1\pm0.7$ (stat.) ±1.1 (sys.) at $y=0$.

The $\Lambda,\bar{\Lambda}$ feed-down corrections reduce this yield by 17.5% [23] when performed in accordance with the PHENIX $\Lambda-$results [24] at 130 GeV, but the amount of stopping remains significant, although a factor of about 4 smaller as compared to Pb-Pb at the highest SPS energy. (A corresponding STAR result [25] for $y=0$ at 130 GeV does not yet include the feed-down correction). Many of the available numerical microscopic models encounter difficulties to predict the net-proton yield in the central midrapidity valley of the distribution, together with the broad peaks at the detected positions.

Here I interpret the data in the nonequilibrium-statistical Relativistic Diffusion Model. The net baryon rapidity distribution at RHIC energies emerges from a superposition of the beamlike nonequilibrium components that are broadened in rapidity space through diffusion due to soft (hadronic, low $p_\perp$) collisions and particle creations, and a statistical equilibrium (thermal) component at midrapidity that arises from hard (partonic, high $p_\perp$) processes [26].

At RHIC energies, the underlying distribution functions turn out to be fairly well separated in rapidity space. Since the transverse degrees of freedom are in (or very close to) thermal equilibrium, they are expected to decouple from the longitudinal ones. The time evolution of the distribution functions is then governed by a Fokker-Planck [27] equation (FPE) in rapidity space [14,16,18,28,29,15,26]. In the more general case of nonextensive (nonadditive) statistics [21] that accounts for long-range interactions and violations of Boltzmann's Stoßzahlansatz [18,28,20] as well as for non-Markovian memory (strong coupling) effects [19,20], the resulting FPE for the rapidity distribution function $R(y,t)$ in the center-of-mass frame is [26]

$$\frac{\partial}{\partial t}[R(y,t)]^\mu = -\frac{\partial}{\partial y}[J(y)[R(y,t)]^\mu] + D(t)\frac{\partial^2}{\partial y^2}[R(y,t)]^\nu. \tag{1}$$

Here, the rapidity diffusion coefficient $D(t)$ may in general be time dependent, although I will use a constant D_y in most of the applications in this work. It accounts for the broadening of the rapidity distributions due to interactions and particle creations, and it is related to the drift term $J(y)$ by means of a dissipation-fluctuation theorem which will be used to actually calculate D_y. The drift $J(y)$ determines the shift of the mean rapidities towards the central value, and I shall discuss linear and nonlinear forms of this drift function.

In derivations of generalized FPE's from the Boltzmann equation, a nonlinear equation ($\mu,\nu\neq1$; nonlinear drift function) could in principle be traced back to the nonlinearities in the transition probabilities between single-particle states [30]. However, this would not yet include non-Markovian effects. Instead, Eq. (1) offers the possibility to describe strong-coupling systems that are beyond the realm of the Boltzmann equation.

Since the norm of the rapidity distribution has to be conserved, $\mu=1$ is required here. It is convenient to introduce a nonextensivity parameter that governs the shape of the power-law equilibrium distribution, $q=2-\nu$ [21]. In statistical equilibrium, transverse mass spectra and transverse momentum fluctuations in relativistic systems at SPS-energies $\sqrt{s_{NN}}=17.3$ GeV require values of q very slightly above one, typically $q=1.038$ for produced pions in Pb-Pb [20]. For $q\rightarrow1$, the equilibrium distribution converges to the exponential Boltzmann form, whereas for larger values of q (with $q<1.5$) significantly broader equilibrium distributions are obtained, and the time evolution towards them becomes superdiffusive [21,31].

To study rapidity distributions in multiparticle systems at RHIC energies in a nonequilibrium-statistical framework [14,16,18,28,29,26], I start with $q=\nu=1$ corresponding to the standard FPE. For a linear drift function

$$J(y) = (y_{eq}-y)/\tau_y \tag{2}$$

with the rapidity relaxation time τ_y, this is the so-called Uhlenbeck-Ornstein process [32], applied to the relativistic invariant rapidity. The equilibrium value is $y_{eq}=0$ in the

center-of-mass for symmetric systems, whereas y_{eq} is calculated from the given masses and momenta for asymmetric systems. Using δ-function initial conditions at the beam rapidities $\pm y_b$ (± 5.36 at $p=100$ GeV/c per nucleon), the equation has analytical Gaussian solutions. The mean values shift in time towards the equilibrium value according to

$$\langle y_{1,2}(t)\rangle = y_{eq}[1-\exp(-2t/\tau_y)] \pm y_b \exp(-t/\tau_y). \quad (3)$$

For a constant diffusion coefficient D_y, the variances of both distributions have the well-known simple form

$$\sigma^2_{1,2}(t) = D_y \tau_y [1-\exp(-2t/\tau_y)], \quad (4)$$

whereas for a time-dependent diffusion coefficient $D_y(t)$ that accounts for collective (multiparticle) and memory effects the analytical expression for the variances becomes more involved [19]. At short times $t/\tau_y \ll 1$, a statistical description is of limited validity due to the small number of interactions. A kinematical cutoff prevents the diffusion into the unphysical region $|y| > y_b$. For larger values of t/τ_y, the system comes closer to statistical equilibrium such that the FPE is valid.

Since the equation is linear, a superposition of the distribution functions [14] emerging from $R_{1,2}(y, t=0) = \delta(y \mp y_b)$,

$$R(y,t) = \frac{1}{2\sqrt{[2\pi\sigma_1^2(t)]}} \exp\left[-\frac{(y-\langle y_1(t)\rangle)^2}{2\sigma_1^2}\right] + \frac{1}{2\sqrt{[2\pi\sigma_2^2(t)]}} \exp\left[-\frac{(y-\langle y_2(t)\rangle)^2}{2\sigma_2^2}\right], \quad (5)$$

yields the exact solution (normalized to 1). With the total number of net baryons (or protons, depending on the experimental results) N_1+N_2 the rapidity density distribution of net baryons (protons) becomes

$$\frac{dN(y, t=\tau_{int})}{dy} = N_1 R_1(y, \tau_{int}) + N_2 R_2(y, \tau_{int}). \quad (6)$$

The value of t/τ_y at the interaction time $t=\tau_{int}$ [the final time in the integration of Eq. (1)] is determined by the peak positions [14] of the experimental distributions. The same approach has also been applied successfully by Biyajima *et al.* to produced particles at RHIC energies [15], although the initial conditions are less straightforward for produced particles, as compared to participant baryons (they use δ-function initial conditions also for produced hadrons).

The microscopic physics is contained in the diffusion coefficient. Macroscopically, the transport coefficients are related to each other in the weak-coupling limit (D_y^w) through the dissipation-fluctuation theorem (Einstein relation) with the equilibrium temperature T,

$$D_y^w = \alpha \cdot T \simeq f(\tau_y, T). \quad (7)$$

In Ref. [14] I have obtained the analytical result for D_y^w as function of T and τ_y from the condition that the stationary solution of Eq. (1) is equated with a Gaussian approximation to the thermal equilibrium distribution in y space (which is not exactly Gaussian, but very close to it) as

$$D_y^w(\tau_y, T) = \frac{1}{2\pi\tau_y}\left\{C(\sqrt{s}, T)\cdot\left[1+2\frac{T}{m}+2\left(\frac{T}{m}\right)^2\right]\right\}^{-2} \times \exp\left(\frac{2m}{T}\right) \quad (8)$$

with $C(\sqrt{s}, T)$ given in Ref. [16] in closed form: for a given equilibrium distribution, the rapidity diffusion coefficient is then determined by the dissipative constant τ_y. The proton mass is m, and $C(\sqrt{s}, T)$ ensures that the corresponding thermal distribution function R_{th} is normalized to 1 for each temperature T

$$\int_{-\infty}^{+\infty} R_{th}(y)dy = 1. \quad (9)$$

This yields

$$C(\sqrt{s}, T) = y_b\left[\int_{-\infty}^{+\infty}[1+2\chi_T(y)+2\chi_T(y)^2]\exp\left(\frac{-1}{\chi_T(y)}\right)dy\right]^{-1} \quad (10)$$

with the beam rapidity y_b in the center of mass, and

$$\chi_T(y) = \frac{T}{m\cosh(y)}. \quad (11)$$

(Note that in Ref. [16] the result is written for the beam rapidity in the laboratory system $y_1=5.83$ at the SPS energy for Pb-Pb, corresponding here to $y_b=\pm 2.195$ in the center of mass).

At fixed beam rapidity y_b, the diffusion coefficient displays the expected behavior, namely, it rises with increasing temperature of the corresponding equilibrium distribution as in the Einstein relation; the rise is almost linear with T. This allows to maintain the linearity of the model and hence, to solve the FPE analytically, although small corrections are to be expected. They cause minor deviations in the calculated rapidity distributions that are within the size of the error bars of the experimental data at SPS energies.

IV. STRONG-COUPLING DIFFUSION: MEMORY EFFECTS

In the linear model, net baryon rapidity spectra at low SIS energies (about 1 GeV per particle) are well reproduced, whereas at AGS and SPS energies I find discrepancies [16] to the data that rise strongly with $\sqrt{s}$. The origin are most likely strong-coupling effects at high energy: the time between two subsequent interactions becomes smaller than the duration of an individual interaction, such that the system becomes non-Markovian and develops memory effects. In a schematic approach that serves to outline the effect analytically, one may account for the system memory by a time-dependent diffusion coefficient through a relaxation ansatz

$$\frac{\partial D_y(t)}{\partial t} = -\frac{1}{\tau_s}[D_y(t) - D_y^w]. \quad (12)$$

Here the diffusion coefficient for weak coupling D_y^w is approached for times $t \gg \tau_s$ larger than the time τ_s that is characteristic for strong coupling—when all secondary particles have been created. D_y^w is well defined in terms of the temperature of the corresponding equilibrium distribution, and the particle mass as discussed above. However, for short times in the initial phase of the collision before and during particle production, the strong-coupling diffusion coefficient D_y^s dominates and enhances the diffusion in y space beyond the weak-coupling value. This enhancement rises strongly with incident energy as shown in Ref. [16]. It is decisive for a proper representation of the available data for relativistic heavy-ion collisions at and beyond SPS energies. The relaxation equation for the rapidity diffusion coefficient with the strong-coupling value D_y^s as an initial condition can be solved as

$$D_y(t) = D_y^w\left[1 - \exp\left(-\frac{t}{\tau_s}\right)\right] + D_y^s \exp\left(-\frac{t}{\tau_s}\right). \quad (13)$$

A lower limit for the characteristic time for strong coupling τ_s can be estimated from the time delay of particle production due to quantum coherence [33] which yields about 0.4 fm/c at SPS energies, or simply from the uncertainty principle, which gives about the same value for a pion. The strong-coupling time τ_s is, however, much larger since it refers to many particles that are created from the available relativistic energy. The transverse energy relaxation time [13]—which is of the order of, but slightly smaller than the interaction time at SPS energies—gives a reasonable estimate for the strong-coupling time such that

$$\tau_s < \tau_{int} < \tau_y \quad (14)$$

at SPS energies. Not much is presently known about the strong-coupling diffusion coefficient D_y^s except that it is significantly larger than its weak-coupling counterpart at these energies. Unlike D_y^w, it cannot be derived from the known equilibrium distribution. Moreover, energy and momentum conservations are not fulfilled in the strong-coupling phase of the collision. Leaving a microscopic model to the future, I presently adjust in the linear model $D_y(t=\tau_{int})$ to the data as outlined in the following section. Due to the strong coupling at short times $t/\tau_y \ll 1$, D_y is initially far above the weak-coupling value D_y^w (8), and it remains there throughout the interaction time at SPS energies, even though it drops slightly until freeze-out occurs. The corresponding variance in rapidity space is obtained analytically through a solution of the corresponding differential equation for the variances with the time-dependent diffusion coefficient (13) contained in the inhomogeneity

$$\frac{d}{dt}\sigma_y^2(t) + 2\sigma_y^2(t) = 2D_y(t)\tau_y. \quad (15)$$

It can be written as a sum of weak- and strong-coupling contributions, respectively,

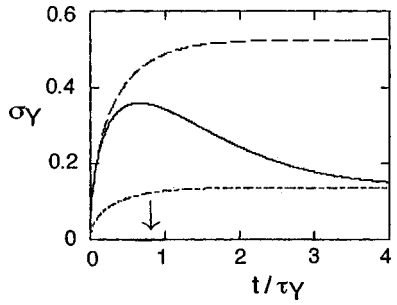

FIG. 2. Standard deviations $\sigma_Y(t)$ of the solutions of the Fokker-Planck equation that build up the Pb-Pb baryon rapidity distribution at SPS momenta of 158 GeV/c per particle in Y space (Fig. 1). The upper curve is the strong-coupling result. Due to particle creation, the actual fluctuations (middle curve) gradually approach the weak-coupling result, lower curve. The interaction time $\tau_{\rm int}/\tau_y$ (arrow) approximately corresponds to the maximum of the fluctuations in rapidity space.

$$\sigma_y^2(t) = \sigma_w^2(t) + \sigma_s^2(t) \quad (16)$$

with

$$\sigma_w^2(t) = D_y^w \tau_y \exp(-2t/\tau_y)\left\{[\exp(2t/\tau_y) - 1] + \frac{2\tau_s}{\tau_y - 2\tau_s}\left[\exp\left(-t/\tau_y\frac{\tau_y - 2\tau_s}{\tau_s}\right) - 1\right]\right\} \quad (17)$$

and

$$\sigma_s^2(t) = D_y^s \tau_y \exp(-2t/\tau_y)\left[\frac{-2\tau_s}{\tau_y - 2\tau_s}\right] \times\left[\exp\left(-t/\tau_y\frac{\tau_y - 2\tau_s}{\tau_s}\right) - 1\right]. \quad (18)$$

In the limit of $\tau_s \to 0$ the fluctuations due to strong coupling vanish, and the remaining weak-coupling result for the variance of the rapidity distribution function attains the familiar form (4)

$$\sigma_y^2(t) \to D_y^w \tau_y[1 - \exp(-2t/\tau_y)] \quad \text{for } \tau_s \to 0. \quad (19)$$

Results for the standard deviations in Y space ($Y = y/y_b$) of the superposed FPE solutions (5) that build up the baryon rapidity distributions in the relativistic system 158 GeV/c per nucleon Pb-Pb are shown in Fig. 2. The strong-coupling value (upper curve) would persist if no particles were created. Due to particle creation, the actual fluctuations pass a maximum and gradually approach the weak-coupling result for large times. The interaction time (here for a central collision) corresponds approximately to the maximum: freeze-out occurs for large fluctuations in rapidity at SPS energies and beyond.

V. FROM SPS TO RHIC ENERGIES

At SPS energies [34], the discrepancy between weak-coupling result and data has recently been confirmed independently in a numerical calculation [18,28] based on a nonlinear drift

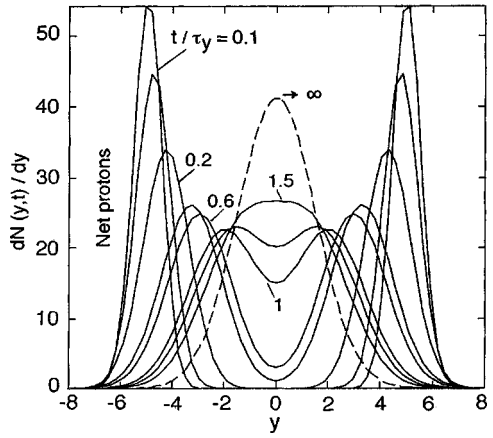

FIG. 3. Analytical solutions of the Relativistic Diffusion Model for various values of t/τ_y representing the diffusive time evolution of the baryonic system (here: net protons) due to interactions and particle creations for central Au-Au at RHIC energies $\sqrt{s_{NN}}$ =200 GeV. Here the net-proton content is 136 protons. This subsystem remains in a nonequilibrium state in the actual experiment, cf. Fig. 6.

$$J(y) = -\alpha \cdot m_\perp \sinh(y) \equiv -\alpha \cdot p \qquad (20)$$

with the transverse mass $m_\perp = \sqrt{m^2 + p_\perp^2}$, and the longitudinal momentum $p_\parallel$. Together with the dissipation-fluctuation theorem (7), this yields exactly the Boltzmann distribution as the stationary solution of Eq. (1) for $\nu = q = 1$. The corresponding numerical solution with δ-function initial conditions at the beam rapidities is, however, only approximately correct since the superposition principle is not strictly valid for a nonlinear drift. Still, the numerical result shows almost the same large discrepancy between data and theoretical rapidity distribution as the linear model. In a $q=1$ framework, the net-proton distribution in Pb-Pb at the highest SPS energy requires a rapidity width coefficient $\sqrt{D_y \tau_y}$ that is enhanced beyond the theoretical value (7) by a factor of $g(\sqrt{s}) \simeq 2.6$ due to memory and collective effects [14,16,19], Fig. 1.

Alternatively, a transition to nonextensive statistics [20,21,31] maintaining the weak-coupling diffusion coefficient from Eq. (7) requires a value of q that is significantly larger than one. In an approximate numerical solution of Eq. (1) with the nonlinear drift (20), $q=1.25$ has been determined for the net-proton rapidity distribution in Pb-Pb collisions at the SPS [18,28]. The only free parameter is q, whereas in the linear $q=1$ case the strong-coupling enhancement of D_y beyond Eq. (7) is the only parameter.

This value of q in the nonlinear model is considerably larger than the result $q(\sqrt{s_{NN}}) = 1.12$ extrapolated from Wilk *et al.* [29] at the SPS energy $\sqrt{s_{NN}} = 17.3$ GeV. Here, the relativistic diffusion approach is applied to produced particles in proton-antiproton collisions in the energy range $\sqrt{s}$ =53 GeV–1800 GeV, and used to predict LHC results. The nonlinearity $q>1$ appears to be an essential feature of the $p\bar{p}$ data. The larger value of q in heavy systems as compared to $p\bar{p}$ at the same NN-center-of-mass energy emphasizes the increasing superdiffusive effect of multiparticle collisions

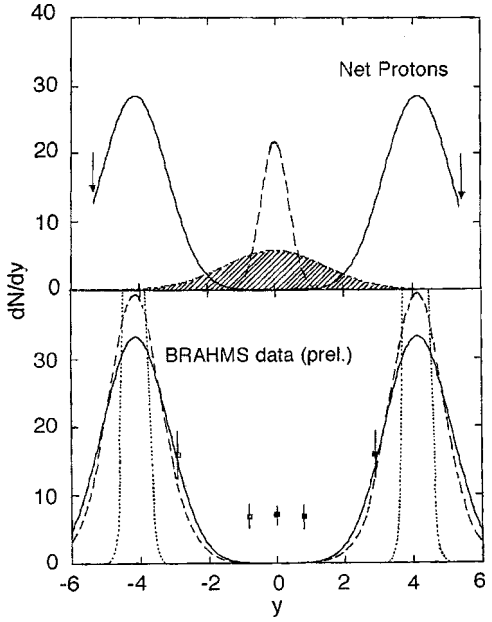

FIG. 4. Nonequilibrium contributions to the net-proton rapidity spectra of central Au-Au at $\sqrt{s_{NN}}=200$ GeV in the RDM with an equilibrium temperature of $T=170$ MeV (bottom). The solid curve is obtained in the linear model ($q=1$). Its width is ("anomalously") enhanced as compared to the theoretical weak-coupling value (dotted curves) by $g(\sqrt{s})=3.7$ due to multiparticle effects [16,19] according to the preliminary BRAHMS data [23], squares. The net-proton content is 158. The dashed curve corresponds to $q=1.4$ and $\langle m_\perp \rangle = 1.2$ GeVin the nonlinear model. Reasonable agreement with the midrapidity data requires that 14% of the net protons reach local thermal equilibrium in a discontinuous transition, top (dashed curve, thermal equilibrium result for 22 protons; shaded area, broadening due to multiparticle effects with $g(\sqrt{s})=3.7$).

both between participants, and between participants and produced particles. It is, however, conceivable that both a violation of Eq. (7) due to memory effects, and $q>1$ have to be considered in a complete description.

The Au−Au system at RHIC energies is then investigated first in the linear $q=1$ model for central collisions (10% of the cross section). Based on the experience at AGS and SPS energies [14,16,19], it is expected that the nonequilibrium net-proton rapidity spectrum calculated with the weak-coupling dissipation-fluctuation theorem (7) underpredicts the widths of the nonequilibrium fractions of the experimental distribution significantly. At RHIC energies, the precise value of the enhancement due to multiparticle effects remains somewhat uncertain at present since the largest-rapidity experimental points are on the edge of the nonequilibrium distribution [23,35]. Typical solutions of the linear FPE for various values of t/τ_y representing the diffusive time evolution of the baryonic system due to interactions and particle creations are shown in Fig. 3.

In the comparison with the BRAHMS data [23] shown in Fig. 4 (bottom), the temperature $T=170$ MeV is taken from a thermal fit of charged antiparticle-to-particle ratios in the Au−Au system at 200 GeV per nucleon [4,36], and the theoretical value of the rapidity width coefficient calculated from the analytical expression (6) is $\sqrt{D_y \tau_y} = 7.6 \times 10^{-2}$. The

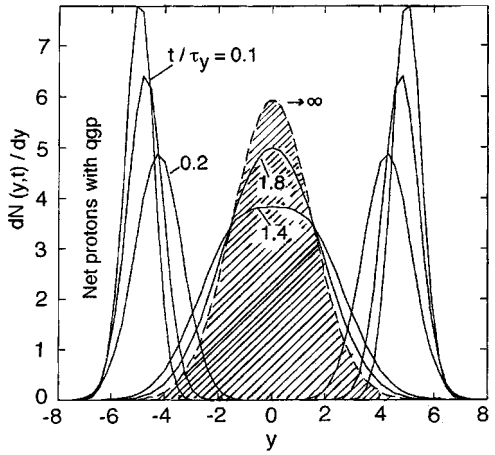

FIG. 5. Analytical solutions of the Relativistic Diffusion Model for various values of t/τ_y representing the time evolution of a local subsystem of net protons in central Au-Au at RHIC energies $\sqrt{s_{NN}}$ = 200 GeV with a sudden enhancement of the number of degrees of freedom due to deconfinement, and the subsequent fast local equilibration. The net-proton content of this local subsystem is 22. The shaded area is the local equilibrium distribution centered at midrapidity.

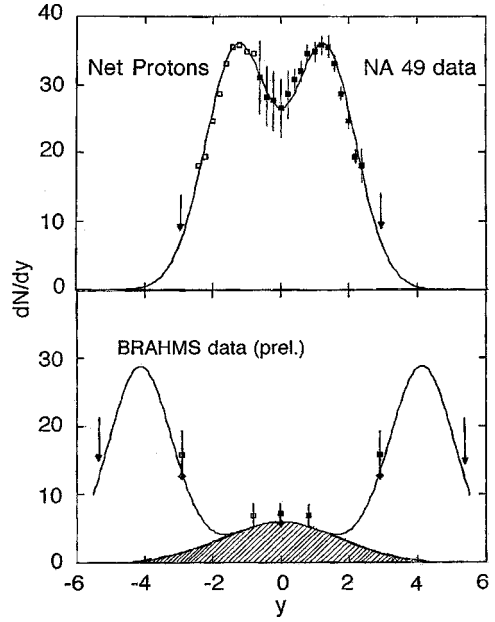

FIG. 6. Net-proton rapidity spectra for central collisions of Au-Au at $\sqrt{s_{NN}}$=200 GeV consist of two nonequilibrium components (solid peaks, bottom; 136 protons) plus a local equilibrium contribution at T=170 MeV. The shaded area shows its broadening due to collective (multiparticle) effects by the same factor $g(\sqrt{s})$ =3.7 as the nonequilibrium fractions. After hadronization, it contains $Z_{eq} \simeq 22$ protons. Superposition creates the flat valley near midrapidity (bottom) in agreement with the preliminary BRAHMS data points [23]. Diamonds include Λ feed-down corrections at y =0 (17.5%) and y=2.9 (20%), respectively. Arrows indicate the beam rapidities $\pm y_b$. At SPS energies (top), NA49 data [38] for central Pb-Pb events (5%) including Λ feed-down corrections are compared with the pure nonequilibrium result of the linear model [14,19]. Here, the net-proton content is 164.

weak-coupling nonequilibrium distributions without enhancement due to multiparticle effects (dotted curves in Fig. 4) are by far too narrow to represent the data, justifying the term "anomalous" for the experimental result.

The calculated distributions become even slightly narrower when T is lowered in order to account for the fact that the equilibrium temperature in the diffusion model should be associated with the kinetic freeze-out temperature (which is not yet precisely known at RHIC), rather than the chemical freeze-out temperature. As has been discussed in Ref. [16], the weak-coupling rapidity diffusion coefficient is proportional to the temperature as in the theory of Brownian motion [37], $D_y \propto T/\tau_y$. Hence, lowering the temperature by 40 MeV reduces the widths of the nonequilibrium distributions by 12%—which is hardly visible on the scale of Fig. 4.

It was shown in Ref. [18] for SPS results that the discrepancy between nonequilibrium weak-coupling result and data persists in case of the nonlinear drift (20) that yields the exact Boltzmann-Gibbs equilibrium solution for q=1,

$$E\frac{d^3N}{d^3p} = \frac{d^3N}{dy \cdot m_\perp dm_\perp d\phi} \propto E \cdot \exp(-E/T). \qquad (21)$$

Hence, it is expected that the nonlinear drift (20) does not improve the situation in the q=1 case at RHIC energies.

Instead, an enhancement of the weak-coupling rapidity width coefficient by a factor of $g(\sqrt{s}) \simeq 3.7$ due to collective and memory effects in the system corresponding to a violation of Eq. (7) yields a good reproduction of the nonequilibrium contributions with τ_{int}/τ_y=0.26. However, the midrapidity valley that is present in the data is completely absent in the extensive nonequilibrium q=1 case, solid curves in Fig. 4 (bottom).

This remains true in the nonextensive case ($1<q<1.5$), with an approximate distribution function [18,21,26,28,29,31] that is given by a linear superposition of power-law solutions of Eq. (1),

$$R_{1,2}(y,t) = \left[1 - (1-q)\frac{m_\perp}{T}\cosh(y - \langle y_{1,2}(t)\rangle)\right]^{1/1-q}. \qquad (22)$$

The dashed curves in Fig. 4 (bottom) show the result for q =1.4, T=170 MeV, and a mean transverse mass $\langle m_\perp \rangle$ =1.2 GeV. This solution is far from the nonextensive equilibrium distribution which would be reached for $\langle y_{1,2}(t\to\infty)\rangle = y_{eq}$, and it is significantly below the midrapidity data. The result is even worse for larger values of $m_\perp$. In contrast, the Pb-Pb data at SPS energies [38] are well described both in the linear model [14] (Fig. 6, top) and in the nonlinear case (cf. Ref. [18] for results with a time-dependent temperature and an integration over transverse mass).

VI. LOCAL DECONFINEMENT AT RHIC

It turns out, however, that the RHIC data can be interpreted rather precisely in the linear q=1 framework with the

conjecture that a fraction of $Z_{eq} \simeq 22$ net protons near midrapidity reaches local statistical equilibrium in the longitudinal degrees of freedom, Figs. 4(top) and 5. The variance of the equilibrium distribution $R_{eq}(y)$ at midrapidity is broadened as compared to the Boltzmann result due to collective (multiparticle) effects by the same factor that enhances the theoretical weak-coupling diffusion coefficient derived from Eq. (7), shaded areas in Figs. 4 and 5. This may correspond to a longitudinal expansion (flow) velocity of the locally equilibrated subsystem as accounted for in hydrodynamical descriptions. In the nonextensive model, the corresponding local equilibrium distribution is broadened (blue shifted) according to $q \simeq 1.4$. Here the enhanced value of q appears as a convenient parametrization of collective expansion ("longitudinal flow").

Microscopically, the baryon transport over 4–5 units of rapidity to the equilibrated midrapidity region is not only due to hard processes acting on single valence (di)quarks that are described by perturbative QCD, since this yields insufficient stopping. Instead, additional processes such as the nonperturbative gluon junction mechanism [39] are necessary to produce the observed central valley. This may lead to substantial stopping even at LHC energies where the separation of nonequilibrium and equilibrium net baryon fractions in rapidity space is expected to be even better than at RHIC. In the late thermalization stage [40], nonperturbative approaches to QCD thermodynamics are expected to be important.

Recent work indicates that one may account for the observed stopping in heavy-ion collisions at SPS and RHIC energies with string-model parameters determined from hadron-hadron collisions [41]. If this was confirmed, the corresponding rapidity distributions would not be considered to be anomalous from a microscopic point of view. However, this view does not offer a distinction between nonequilibrium and equilibrium contributions to the net baryon rapidity spectra, which both exist at RHIC energies, and are anomalously broadened.

Macroscopically, the complete solution of Eq. (1) in the $q=1$ case is a linear superposition of nonequilibrium and local equilibrium distributions (Fig. 6, bottom)

$$R(y, t=\tau_{int}) = R_1(y, \tau_{int}) + R_2(y, \tau_{int}) + R_{eq}^{loc}(y) \qquad (23)$$

with the same enhancement factor $g(\sqrt{s})$ due to multiparticle (collective) effects for all three distributions. The net-baryon rapidity distribution becomes

$$\frac{dN(y, t=\tau_{int})}{dy} = N_1 R_1(y, \tau_{int}) + N_2 R_2(y, \tau_{int}) + N_{eq} R_{eq}^{loc}(y) \qquad (24)$$

with the number N_{eq} of net baryons (here: net protons) in local equilibrium near mid rapidity, and $N_1+N_2+N_{eq}$ equal to the total number of net baryons (158 net protons for central Au-Au). This yields a good representation of the preliminary BRAHMS data [23]. (In the $q>1$ case, the corresponding solution is questionable because the superposition principle is violated). Based on Eq. (24), the transition from net-proton rapidity spectra with a central plateau in Pb-Pb at the lower SPS energies [19], via a double-humped distribution at the maximum SPS energy [14,18,19,28,38] to the central valley at RHIC [23,26] is well understood. It has not yet been possible to identify a locally equilibrated subsystem of net baryons at midrapidity below RHIC energies, although it cannot be excluded that it exists. At SPS energies, the data [38] are well described by the nonequilibrium distributions, and it is much more difficult (and probably impossible) to identify a locally equilibrated component because the relevant rapidity region is comparatively small, and an equilibrated contribution cannot be separated from the nonequilibrium components in rapidity space. In $p\overline{p}$ collisions at $\sqrt{s}=53-900$ GeV, no convincing signatures of a phase transition were found [42].

Most remarkably, Figs. 4–6 suggest that in central Au−Au collisions at $\sqrt{s_{NN}}=200$ GeV there is no continuous transition from the nonequilibrium to the equilibrium contribution in net-proton rapidity spectra as function of time. The central valley in net-proton rapidity spectra at RHIC energies could thus be used as an indicator for partonic processes that lead to a baryon transfer over more than four units of rapidity, and for quark-gluon plasma formation. The discontinuity may well be due to a sudden enhancement in the number of degrees of freedom as encountered in the deconfinement of participant partons, which enforces a very rapid local equilibration in a fraction of the system as indicated in Figs. 4 and 5 through a discontinuity in the time evolution of the solutions of the FPE, which are afterwards very close to the equilibrium result. Here, the sudden enhancement in the number of degrees of freedom by a factor of about 6 in the quark-gluon plasma as compared to the hadronic phase [2] is modeled by a corresponding increase in time, Fig. 5.

The linear RDM with three sources [26] including a local equilibrium fraction near midrapidity has recently also been adopted by Biyajima *et al.* [22] for produced particles in analyses of BRAHMS [43] and PHOBOS [44] pseudorapidity data at $\sqrt{s}=130$ GeV and 200 GeV, using the proper Jacobian to transform from y to $\eta=-\ln\tan(\theta/2)$. In particular, the PHOBOS data [44] at 130 (200) GeV and 0–6% centrality are well reproduced with 3134 (3858) charged hadrons in the central source indicative of an equilibrated qgp, whereas only 896 (1102) charged hadrons reside in the nonequilibrated fragmentation regions.

These very recent results for produced charged hadrons are, however, still somewhat ambiguous in view of (1) the uncertainties regarding the initial conditions for produced particles in rapidity space and (2) the difficulties to clearly separate fragmentation and central regions for produced particles. Nevertheless, the RDM analyses of produced hadrons by Biyajima *et al.* [42] provide additional evidence for local equilibrium near midrapidity.

VII. CONCLUSION

To conclude, I have interpreted recent results for central Au-Au collisions at RHIC energies in a Relativistic Diffusion Model (RDM) for multiparticle interactions based on the interplay of nonequilibrium and local equilibrium ("thermal") solutions. In the linear version of the model, analytical results for the rapidity distribution of net protons in central

collisions have been obtained. The anomalous enhancement of the diffusion in rapidity space as compared to the expectation from the weak-coupling dissipation-fluctuation theorem due to high-energy multiparticle effects has been discussed using extensive and nonextensive statistics.

A significant fraction of about 14% of the net protons reaches local statistical equilibrium in a fast and discontinuous transition which is likely to indicate parton deconfinement. The precise amount of protons in local equilibrium is related to the experimental value of the rapidity density close to $y=0$ and hence, possible changes in the final data will affect the percentage. It has not yet been possible to isolate a corresponding fraction of longitudinally equilibrated net protons in the Pb-Pb system at SPS energies. Since no signatures of a transition to the quark-gluon plasma have been observed in $p\bar{p}$ collisions, quark-matter formation is clearly a genuine many-body effect occurring only in heavy systems at sufficiently high-energy density. Consequently, a detailed investigation of the flat midrapidity valley found at RHIC, and of its energy dependence is very promising.

[1] H. Gutbrod, J. Aichelin, and K. Werner (eds.), Nucl. Phys. **A715**, 3c-930c (2003).
[2] D. J. Schwarz, Ann. Phys. (Leipzig) **12**, 220 (2003).
[3] R. Hagedorn, Nucl. Phys. **B24**, 93 (1970); Nuovo Cimento, Suppl. **3**, 147 (1965).
[4] F. Becattini *et al.*, Phys. Rev. C **64**, 024901 (2001).
[5] P. Braun-Munzinger, D. Magestro, K. Redlich, and J. Stachel, Phys. Lett. B **518**, 41 (2001).
[6] T. Matsui and H. Satz, Phys. Lett. B **178**, 416 (1986).
[7] K. Reygers, PHENIX Collaboration, GPS meeting Tübingen 3, 2003.
[8] B. B. Back *et al.*, PHOBOS Collaboration, Phys. Rev. Lett. **91**, 072302 (2003).
[9] S. S. Adler *et al.*, PHENIX Collaboration, Phys. Rev. Lett. **91**, 072303 (2003).
[10] J. Adams *et al.*, STAR Collaboration, Phys. Rev. Lett. **91**, 072304 (2003).
[11] I. Arsene *et al.*, BRAHMS Collaboration, Phys. Rev. Lett. **91**, 072305 (2003).
[12] C. Adler *et al.*, STAR Collaboration, Phys. Rev. Lett. **90**, 082302 (2003).
[13] G. Wolschin, Z. Phys. A **355**, 301 (1996).
[14] G. Wolschin, Eur. Phys. J. A **5**, 85 (1999).
[15] M. Biyajima, M. Ide, T. Mizoguchi, and N. Suzuki, Prog. Theor. Phys. **108**, 559 (2002); **109**, 151 (2003).
[16] G. Wolschin, Europhys. Lett. **47**, 30 (1999).
[17] M. Biyajima and T. Mizoguchi, Prog. Theor. Phys. **109**, 483 (2003); M. Ide, M. Biyajima, and T. Mizoguchi, nucl-th/0302003.
[18] A. Lavagno, Physica A **305**, 238 (2002).
[19] G. Wolschin, Pramana **60**, 1035 (2003).
[20] W. M. Alberico, A. Lavagno, and P. Quarati, Eur. Phys. J. C **12**, 499 (2000).
[21] C. Tsallis, J. Stat. Phys. **52**, 479 (1988); C. Tsallis and D. J. Bukman, Phys. Rev. E **54**, R2197 (1996).
[22] M. Biyajima, M. Ide, M. Kaneyama, T. Mizoguchi, and N. Suzuki, Prog. Theor. Phys. Suppl. (to be published), nucl-th/0309075.
[23] J. H. Lee *et al.*, BRAHMS Collaboration, Nucl. Phys. **A715**, 482c (2003).
[24] K. Adcox *et al.*, PHENIX Collaboration, Phys. Rev. Lett. **89**, 092302 (2002).
[25] C. Adler *et al.*, STAR Collaboration, Phys. Rev. Lett. **87**, 262302 (2001).
[26] G. Wolschin, Phys. Lett. B **569**, 67 (2003); hep-ph/0301004.
[27] N. G. v. Kampen, *Stochastic Processes in Physics and Chemistry* (North Holland, Amsterdam, 1981).
[28] W. M. Alberico, A. Lavagno, and P. Quarati, nucl-th/0205044.
[29] M. Rybczyński, Z. Włodarczyk, and G. Wilk, Nucl. Phys. B (Proc. Suppl.) **122A**, 325 (2003); hep-ph/0206157.
[30] G. Wolschin, Phys. Rev. Lett. **48**, 1004 (1982).
[31] G. Wilk and Z. Włodarczyk, Phys. Rev. Lett. **84**, 2770 (2000).
[32] M. Jacobsen, Bernoulli **2**, 271 (1996).
[33] C. Gale, S. Jeon, and J. Kapusta, Nucl. Phys. **A661**, 558c (1999).
[34] S. Margetis *et al.*, NA49 Collaboration, Nucl. Phys. **A590**, 355c (1995).
[35] I. G. Bearden *et al.*, BRAHMS Collaboration, Nucl. Phys. **A715**, 171c (2003).
[36] I. G. Bearden *et al.*, BRAHMS Collaboration, Phys. Rev. Lett. **90**, 102301 (2003).
[37] A. Einstein, Ann. Phys. (Leipzig) **17**, 549 (1905).
[38] H. Appelshäuser *et al.*, NA49 Collaboration, Phys. Rev. Lett. **82**, 2471 (1999).
[39] G. C. Rossi and G. Veneziano, Phys. Rep. **63**, 153 (1980); D. Kharzeev, Phys. Lett. B **378**, 238 (1996); S. E. Vance, M. Gyulassy, and X. N. Wang, *ibid.* **443**, 45 (1998).
[40] J. Berges and J. Cox, Phys. Lett. B **517**, 369 (2001); G. Aarts and J. Berges, Phys. Rev. D **64**, 105010 (2001).
[41] A. Capella, Phys. Lett. B **542**, 65 (2002).
[42] C. Geich-Gimbel, Int. J. Mod. Phys. A **4**, 1527 (1989).
[43] I. G. Bearden *et al.*, BRAHMS Collaboration, Phys. Lett. B **523**, 227 (2001); Phys. Rev. Lett. **88**, 202301 (2002).
[44] B. B. Back *et al.*, PHOBOS Collaboration, Phys. Rev. Lett. **87**, 102303 (2001); R. Noucier *et al.*, PHOBOS Collaboration, nucl-ex/0208003.